Biosensors and Bioelectronics 102 (2018) 464–469

Contents lists available at ScienceDirect

Biosensors and Bioelectronics

journal homepage: www.elsevier.com/locate/bios

Nitration of tyrosine and its effect on DNA hybridization

Seda Nur Topkaya[a,*], Vasfiye Hazal Ozyurt[b], Arif E. Cetin[c], Semih Otles[b]

[a] Department of Analytical Chemistry, Faculty of Pharmacy, İzmir Katip Celebi University, Izmir, Turkey
[b] Department of Food Engineering, Faculty of Engineering, Ege University, Izmir, Turkey
[c] Koch Institute for Integrative Cancer Research, Massachusetts Institute of Technology, Cambridge, USA

ARTICLE INFO

Keywords:
Electrochemical DNA biosensor
DNA hybridization
Protein nitration
3-Nitro-L-tyrosine
Tyrosine
Hybridization indicator

ABSTRACT

One major marker of nitrosative stress is the formation of 3-Nitrotyrosine (3-NT) from Tyrosine (Tyr) by adding a nitro group (-NO_2) with nitrating agents. Nitration of Tyr often causes loss of protein activity and is linked with many diseases. In this article, we detect 3-NT and discriminate it from Tyr with Differential Pulse Voltammetry (DPV) as it is a very important biomarker. We first examined redox (oxidation/reduction) properties and stability of 3-NT in detail. Second, we provided the Tyr and 3-NT discrimination with DPV and compared with the chromatography. We then explored the interaction of 3-NT and DNA oligonucleotides. Our findings demonstrate that 3-NT can be used as a new electrochemical indicator, which is able to detect hybridization of probe (single stranded DNA-ssDNA) and hybrid (double stranded DNA-dsDNA) both via 3-NT reduction and guanine oxidation signal changes at the same time. The signal differences enabled us to distinguish ssDNA and dsDNA without using a label or a tag. Moreover, we achieved to detect hybridization of DNA by using the reduction signal of 3-NT obtained at −0.4 V vs. Ag/AgCl. More importantly, we observed the changes of the reduction signals of 3-NT after the interaction of probe and hybrid sequences. We showed that 3-NT signal decreases more with hybrid than the probe. Our platform, for the first time, demonstrates the detection of hybridization both guanine oxidation and indicator reduction signal changes at the same time. Moreover, we, for the first time, demonstrated the interaction between 3-NT and DNA.

1. Introduction

Protein tyrosine nitration is a post-translational modification that occurs under the action of nitrating agents such as nitrate, nitrit and derivatives of peroxynitrit (Chen and Chen, 2012; Degendorfer et al., 2016). Aforesaid nitrating agents act as reactive compounds and help the formation of nitric oxide and peroxynitrit, which have been known as reactive nitrogen species (RNS). At physiological pH, RNS can react with a number of biomolecules such as DNA, proteins and lipids (Greenacre and Ischiropoulos, 2001). Tyrosine nitration changes the key properties of the amino acids such as redox potential, hydrophobicity and the values of pKa (Radi, 2013). RNS reacts with Tyrosine (Tyr) to form 3- Nitro-L-tyrosine (3-NT) replacing by hydrogen in the ortho position of the phenolic ring of the Tyr residues with a nitro group (-NO_2). 3-NT is therefore likely not a footprint for peroxynitrite alone but more generally a marker of nitrative stress. Chemical structures and the relationship between Tyr and 3-NT are shown in Fig. 1.

3-NT levels in biological matrices and fluids including plasma, serum, urine, cerebrospinal and synovial fluids have been associated with numerous physiological and pathological conditions such as immunological reactions, psychiatric disorders, cardiovascular and neurodegenerative diseases (Bolner et al., 2016; Daiber and Munzel, 2012; Zhao et al., 2014). A great deal of efforts has been spent to develop methods that accurately and sensitively quantify 3-NT since it can be used as a biomarker of nitrosative stress. The most preferred technique to determine the 3-NT is high-performance liquid chromatography (HPLC) (Teixeira et al., 2017) coupled to ultraviolet–visible (UV–Vis) (Erdal et al., 2008; Kilciksiz et al., 2011; Sharov et al., 2006) and fluorescence detector systems (FLD) (Guo et al., 2009). Recently, mass spectrometry (MS) or tandem mass spectrometry coupled with liquid chromatography (LC-MS/MS) is also introduced due to its ability to detect low concentration levels of analyte (Li et al., 2015; Wang et al., 2007). However, MS requires skilled operators and time consuming sample preparation steps. LC-MS/MS technique is also quite expensive due to the need of isotope labeled analogs of interest. Apart from the chromatographic based methods, other methods exist based on 3-NT detection in tissues and fluids with antibody-based methods, i.e., enzyme-linked immunosorbent assay (ELISA) (Sun et al., 2007; Weber et al., 2012). Generally, ELISA employs antibodies with tagged fluorescent dyes to measure the capture of target antigens. Both

* Corresponding author.
E-mail addresses: sedanur6@gmail.com, sedanur.topkaya@ikc.edu.tr (S.N. Topkaya).

https://doi.org/10.1016/j.bios.2017.11.061
Received 12 August 2017; Received in revised form 15 November 2017; Accepted 22 November 2017
Available online 23 November 2017
0956-5663/ © 2017 Elsevier B.V. All rights reserved.

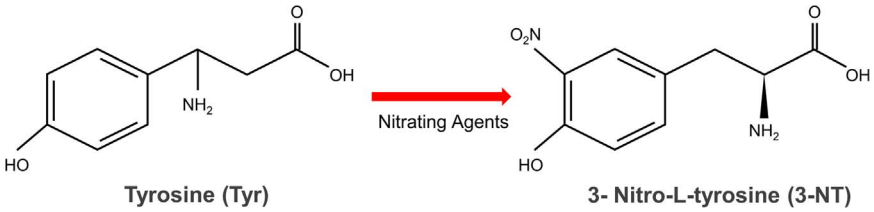

Fig. 1. Tyrosine conversion to 3-Nitro-L-tyrosine under the effect of nitrating agents. In the figure, nitrating agents are NO•; $ONOO^-$;NO^-; $ONOOCO_2^-$; NO_2Cl; NO_3^-; NO_2^-.

chromatographic and antibody-based detection methods have time-consuming extraction steps and/or require expensive standards.

The detection, identification and quantification of a biologically important target molecules and biomarkers, especially at low concentrations can be achieved with electrochemical based biosensor systems (Adhikari et al., 2017; Afkhami et al., 2017; Aghaei et al., 2017; Aghili et al., 2017; Alexander et al., 2017; Arevalo et al., 2017; Mahato et al., 2017). In that sense, electrochemical biosensors can enable highly sensitive, specific, rapid, low-cost and easy to handle detection. Another advantage of using electrochemical biosensors is that they can be miniaturized (lab-on-a-chip devices) and offer robust results compared to the classical analytical techniques such as immunohistochemistry or ELISA. Due to these unique advantages, electrochemical biosensors can successfully provide an efficient and reliable detection for the determination of 3-NT with high sensitivity in a cost-effective manner.

Herein, we aim to detect 3-NT and its interaction with DNA oligonucleotides by using its oxidation/reduction properties with voltammetry. In literature, there are very few studies on the detection of 3-NT with electrochemical techniques (Acar et al., 2016; Richards et al., 2006; Roy et al., 2015). In the present study, we first analyzed oxidation and reduction properties of Tyr and 3-NT and achieved the discrimination with Differential Pulse Voltammetry (DPV). Our electrochemical based results were compared with chromatography of Tyr and 3-NT discrimination, demonstrating that our method provides an easy-to-use (no extraction step), rapid (nearly 1 min) and cost effective detection. More importantly, in addition to clarifying redox properties of 3-NT and its discrimination from Tyr, we for the first time, showed 3-NT's interaction with DNA oligonucleotides. Briefly, electrodes were first activated to provide effective surface area. Then, probe sequences were immobilized onto the electrodes by dipping electrodes into the probe solution. Probe coated electrodes were later interacted with its target sequence to create hybrid form on the surface of electrodes. After obtaining the probe, hybrid (probe + target) on the electrode surfaces, we investigated the effect of 3-NT on DNA sequences. In order to detect the hybridization and interaction events, the changes in the oxidation signal of the guanine bases of DNA at approximately +1.00 V versus Ag/AgCl reference electrode were measured with DPV. Intrinsic electroactivity of guanine bases have been used as an indicator for the direct measurement of nucleic acids in a label-free assay (Dogan-Topal et al., 2009; Kilic et al., 2012; Topkaya et al., 2010). We observed that 3-NT behaves as a '**hybridization indicator**' due to its distinct electrochemical behavior to different strands of DNA. After interaction with 3-NT, guanine oxidation signals of probe signals decreased dramatically whereas hybrid signals remain almost unchanged. The signal differences enabled us to distinguish single stranded DNA (ssDNA-probe) and double stranded DNA (dsDNA-hybrid) without using a label or tag. Moreover, 3-NT reduction signals observed at nearly −0.4 V vs. Ag/AgCl were evaluated and optimized. In this study we, for the first time, showed the detection of hybridization of DNA by using the reduction signal of 3-NT. Interestingly, we observed the changes of the reduction signals of 3-NT after the interaction of probe and hybrid sequences. Hybridization indicators behave distinctly to different strands of DNA, which makes them an ideal candidate for detection of hybridization of DNA apart from the guanine signals. This feature is extremely important in lack of guanine bases during the investigation of sequence, such that indicators provide us an alternative route to detect hybridization.

Redox (oxidation/reduction) properties of 3-NT were first examined. Second, Tyr and 3-NT discrimination was provided with DPV and compared with HPLC. Third, the interaction of 3-NT and DNA oligonucleotides was explored. Last, hybridization was detected via guanine oxidation and 3-NT reduction signals at the same time. Our findings introduced **a new hybridization indicator,** 3-NT to the literature.

2. Materials and methods

2.1. Instruments

DPV measurements were carried out using μ-AUTOLAB Type III-Electrochemical Analysis System (Eco Chemie, Netherlands). Three electrode system consists of a pencil graphite electrode (PGE) as the working electrode, a reference electrode (Ag/AgCl, Model RE-1 BAS, USA), and a platinum wire as the auxiliary electrode. The pencil graphite leads are composite materials containing graphite (~ 65%), clay (~ 30%), and a binder (wax, resins, or high polymer). HB type pencil leads were used which contain equal portions of graphite and clay. The surface area was calculated as 0.255 cm^2 for PGE. HB pencil leads with a length of 60 mm and a diameter of 0.5 mm were employed. Pencil Model T 0.5 mm (Rotring, Germany), was used as a holder for pencil lead (Tombo, Japan), which were purchased from a local bookstore.

Agilent 1200 HPLC apparatus (Agilent Technologies, Germany) equipped with a diode array detector (DAD), a quaternary elution pump, and auto sampler injection system and a temperature-controlled column oven were used. An Inertsil ODS-3 RP-HPLC column (5 μm, 150 × 4.6 mm) and a guard column (10 × 4.6 mm) filled with the same material was chosen.

2.2. Chemicals

Tyrosine ($C_9H_{11}NO_3$) and 3-NT ($C_9H_{10}N_2O_5$) were supplied from Sigma. Stock solution of Tyr and 3-NT (1 mg/mL) was prepared by dissolving a weighed amount in ultrapure water. Diluted concentrations of Tyr and 3-NT were prepared in daily with 0.05 M phosphate buffer containing 20 mM NaCl (PBS, pH 7.4). Other chemicals in analytical reagent grade were supplied from Sigma and Merck.

2.3. Oligonucleotides

HPLC-purified oligonucleotides were purchased as lyophilized powders from TIB-MOLBIOL (Germany). Their base sequences are as follows:

Probe: 5′-TTC GGG GTG TAG CGG TCG TC-3′

Target: 5′-GAC GAC CGC TAC ACC CCG AA-3′

The oligonucleotides stock solutions were prepared in ultrapure water and stored at −20 °C. Diluted solutions of probe were prepared using 0.5 M acetate buffer solution containing 20 mM NaCl (ACB, pH:4.8) and diluted target solutions were prepared using PBS.

2.4. Steps for determination of 3-NT and its interaction with DNA

2.4.1. Electrochemical detection

The steps for the monitoring the interaction are as follows:

Graphite electrode pre-treatment: PGEs were pretreated by applying +1.4 V for 30 s in ACB to create –COOH groups to enhance the adsorptive accumulation of DNA oligonucleotides.

Immobilization of probe-DNA onto the electrode surface and hybridization with complementary target-DNA: The probe was immobilized onto the surface of PGEs with passive adsorption. For this purpose, PGEs were dipped into 5 µg/mL of probe for 20 min. The electrodes were then rinsed with ACB. Hybridization was performed in PBS with 500 mM NaCl containing 7 µg/mL of target sequence for 45 min. DNA modified electrodes were then rinsed 3 times with the hybridization buffer.

Interaction of oligonucleotides with 3-NT: After coating of the electrodes with probe and hybrid DNA oligonucleotides, 15 µg/mL of 3-NT was interacted with the DNA modified electrodes for 30 min. After 10 min, the electrodes were rinsed with PBS.

Signal measurements with DPV: Both guanine and 3-NT oxidation signals were measured by DPV (step potential: 8 mV; modulation amplitude: 80 mV, scan rate of 50 mV/s.) in ACB by scanning from +0.6 V to +1.1 V. The differences of guanine oxidation signals obtained from probe, hybrid, probe+3-NT and hybrid+3-NTcoated PGEs were examined. The reduction signals of 3-NT were observed at nearly −0.4 V by scanning from −0.2 V to −0.5 V.

2.4.2. HPLC based detection

The separation of the standard compounds (T and 3NT) using an Inertsil ODS-3 RP-HPLC column (5 µm, 150 Å ~ 4.6 mm) and a guard column (10 Å ~ 4.6 mm) filled with the same material was done. Tyr and 3NT were separated each other by the procedure described in our previous study (Ozyurt and Otles, 2017). The mixture of 50 mM sodium citrate buffer with pH 3.1% and 8% methanol in 50 mM ACB was used as mobile phases. The wavelengths having the maximum absorbance of Tyr and 3-NT were adjusted to 274 nm and 278 nm, respectively. The chromatogram was plotted mAU (milli absorbance unit) versus min. A schematic for the detection procedure is presented in Fig. 2.

3. Results and discussion

3-NT detection with electrochemical techniques is generally preferred for instrumental simplicity, cost effectivity and portability. In Fig. 3, electrochemical (voltammetry) and chromatographic (HPLC) results are shown.

In Fig. 3A, a voltammogram is shown for the reduction of 3-NT by scanning from −0.2 V to −0.5 V vs. Ag/AgCl in ACB at a scan rate of 50 mV s^{-1}. For this study, the graphite electrodes were activated and then they were dipped into 20 µL of blank, 1 mg/mL Tyr and 3-NT solutions. We observed no signal for blank and Tyr solutions due to lack of reducible groups in their structure. On the other hand, 3-NT reduction signal was obtained nearly at −0.4 V. As stated, the incorporation of a -NO_2 group on the C-3 of the phenolic ring could changes in key properties of the parent amino acid (Radi, 2013). For instance, the pKa values of the phenolic group for Tyr and 3-NT can vary within a protein compared to those of the free amino acids in solution, depending on the polarity of the medium and the influence of neighboring amino acids (Yokoyama et al., 2010). It has been previously shown that 3-NT substantially can be reduced to aminotyrosine in a purely chemical reaction between Fe^{3+} containing heme and a reducing agents under physiological conditions (pH 7.2, 37 °C) (Chen et al., 2008). Our study showed the reduction of 3-NT to aminotyrosine by applying potential without the need for any chemical agents or laborious experimental steps with DPV.

In Fig. 3B, a voltammogram was obtained for the oxidation of Tyr and 3-NT by scanning from +0.4 V to +1.0 V in ACB. Tyr is oxidized at around +0.6 V whereas 3-NT is oxidized at +0.85 V. As clearly seen in the figure, the oxidation signal was shifted from +0.6 V to +0.85 V when the Tyr was nitrated. The reported mechanisms of Tyr oxidation substantially depend on the electrode materials and experimental conditions (Lopes et al., 2014) and was suggested as hydroxyl groups involving the transfer of two protons and two electrons, resulting in the formation of quinone-type products (Kerman et al., 2007). The observed result is due to the -NO_2 group creating local steric restrictions

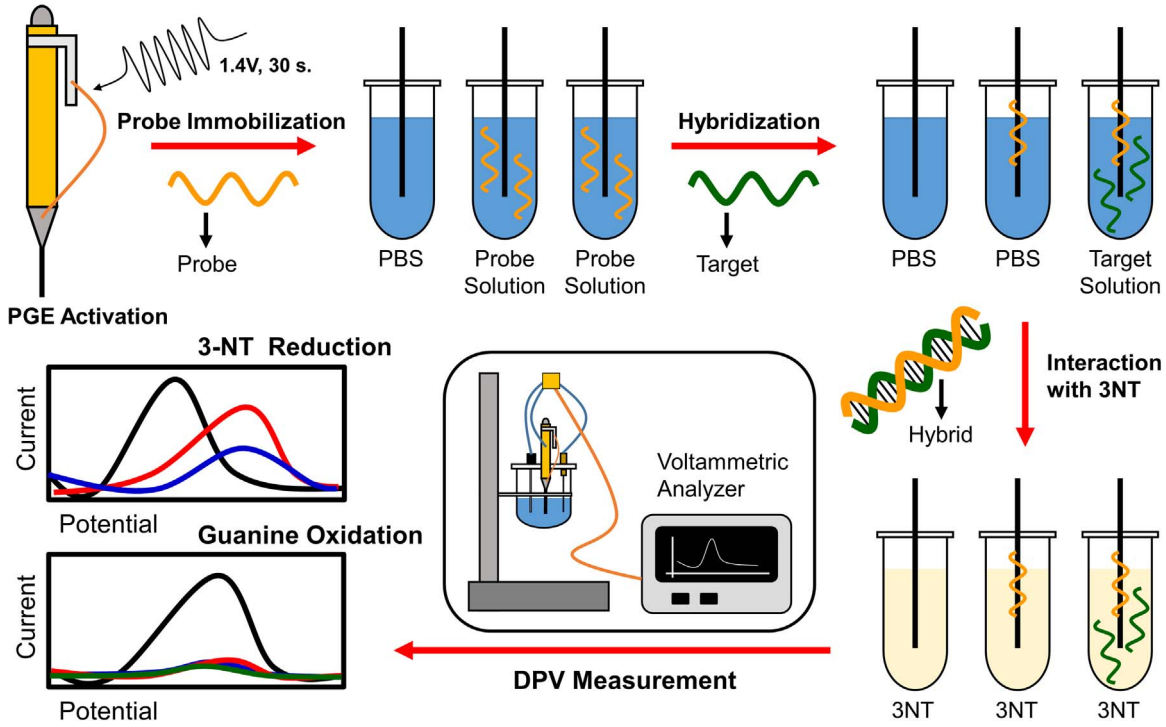

Fig. 2. Schematics of electrochemical detection of interaction between DNA oligonucleotides and 3-NT.

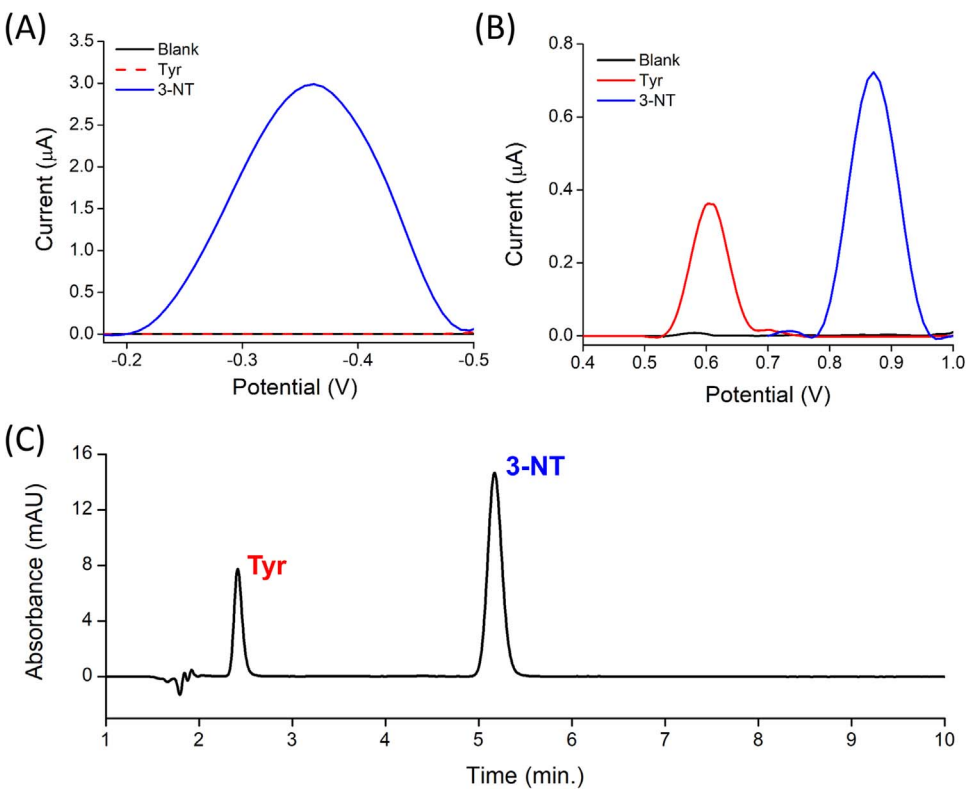

Fig. 3. Discrimination of Tyr and 3-NT via (A) reduction and (B) oxidation signals with voltammetry, and (C) HPLC.

and triggering conformational changes, and impeding tyrosine phosphorylation. As shown in Figs. 3A and B, the signal differences allow discriminating Tyr and 3-NT at the same voltammogram only in seconds.

Fig. 3C represents a typical chromatogram for the discrimination of Tyr and 3-NT. The injection volume of a standard solution mixture containing Tyr and 3-NT was 50 µL. The flow rate was kept at 1 mL/min and the temperature of the column was maintained at 20 °C. The wavelengths for the maximum absorbance of Tyr and 3-NT were adjusted to 274 nm and 278 nm, respectively. The chromatogram was plotted mAU (milli absorbance unit) in time (min). The retention times for Tyr and 3-NT were 2.5 and 5.2 min, respectively. The polarity of Tyr is higher than 3-NT such that it was detected first. Compared to the chromatography results with the electrochemical ones, voltammetry have more advantages, i.e., shorter measurement time (10 min for HPLC, 30 s for DPV). Moreover, potentiostat is 2–3 times cheaper than HPLC. HPLC also requires well-trained professionals, while the voltammetric measurements are easy-to-operate.

In order to optimize the 3-NT concentration, activated electrodes was immersed into 3-NT solution in different concentrations varying from 15 to 100 µg/mL in PBS for 10 min Fig. 4 shows reduction (A) and oxidation (B) signals obtained from different concentrations of 3-NT with DPV in ACB. A well-defined sharp reduction (Fig. 4A) and oxidation (Fig. 4B) peaks were observed. As it seen in Fig. 4, the oxidation/reduction peak currents were increased linearly with the increasing concentration of 3-NT. Calibration curves were recorded for Tyr and 3-NT by plotting the peak maxima of the DPV. The plot of reduction and oxidation peak currents versus the potential was linear with a correlation coefficient of 0.9957 (Fig. 4A, inset) and 0, 9995 (Fig. 4B, inset), respectively. The limit of detection (LOD) values for the developed method was calculated using LOD = 3 s/m equation. In this equation, m is the slope of the calibration curve and s is the standard deviation calculated by regression analysis for S/N = 3. For the reduction of 3-NT, LOD was found to be 244 µg/mL (21.6 µmol in 20 µL sample) with a regression equation y = 0.1106x + 8.9559 with the coefficient of determination (R^2) of 0.9957. For the oxidation of 3-NT, LOD was found as 168 µg/mL (14, 9 µmol in 20 µL sample) with a regression equation y = 0.003706x + 0.2091 with R^2 of 0.9995. Since the sufficiently detectable and more reproducible signals were obtained in the presence of 15 µg/mL 3-NT, it was chosen as the optimum for further studies. The obtained results suggest that the sensitive determination of 3-NT is possible at PGE.

Fig. 5 shows the DPVs obtained for the oxidation of 3-NT at bare and activated PGE in ACB at a scan rate of 50 mV/s. In the experiments, stock solution of 3-NT (1 mg/mL) was prepared by dissolving a weighed amount of the standard substance in ultrapure water. Then, 3-NT solution was diluted to desired concentration with PBS. The oxidation signal of 3-NT was measured at 0.5 h. where its peak potential was observed at +0.85 V. When the same solution is measured at 5 h., 3-NT oxidation signal potential shifted to +0.65 V (less positive values). In addition, the peak current is larger at 0.5 h. than 5 h., i.e., approximately dropped by 85%. In Fig. 5-inset, the photograpgh of the solutions at 0.5 h. and 5 h. are showed. At 5 h., the colorless solution turned into a light yellow color, which is due to the continuous degradation of 3-NT.

Hybridization between complementary single stranded sequences is the most preferred bio-recognition systems compared to enzymes or antibodies due to its stability and assay time. Such specific and sensitive recognition layers acquire unique properties to electrochemical biosensors for point-of-care analysis. In that sense, the detection of specific DNA sequences, epigenetic modifications such as DNA hypermethylation (Topkaya et al., 2012) or DNA mutations (Topkaya et al., 2014) using electrochemical biosensors significantly provide shorter time, better sensitivity and easy-to-operate compared to traditional DNA sequencing methods. For these purposes, interaction between 3-NT and DNA study was performed to investigate the behavior of 3-NT on probe and hybrid to understand how 3-NT interacts with different strands of nucleic acids by evaluating both reduction signal of 3-NT and oxidation signal of guanine bases. Fig. 6 clearly demonstrates the hybridization both 3-NT reduction and guanine oxidation signal. Monitoring the hybridization event with alternative indicators is critical for the sequences without guanine bases.

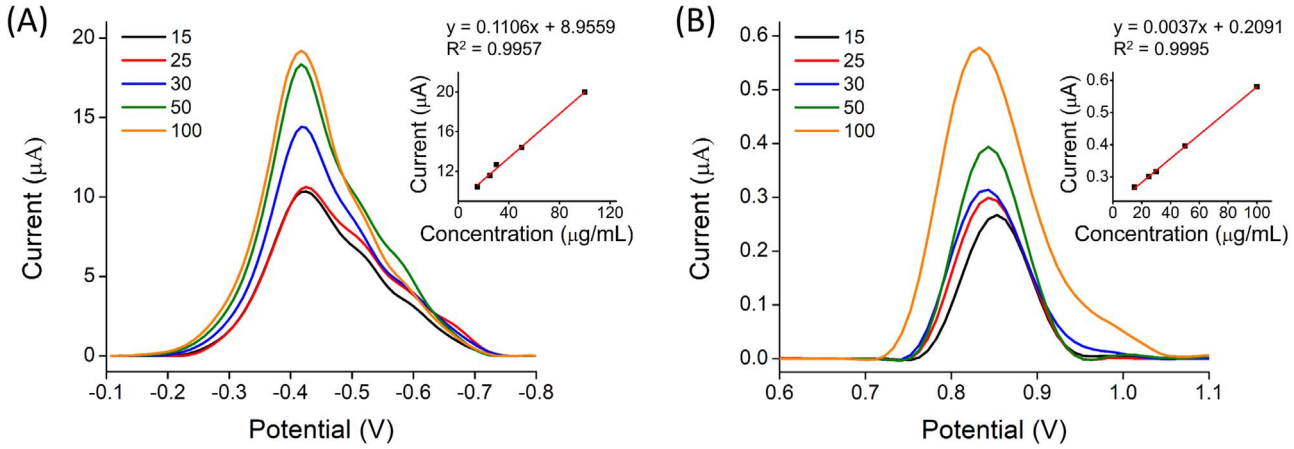

Fig. 4. Voltammogram of (A) reduction and B) oxidation signals for different concentrations of 3-NT ranging from 15 to 100 μg/mL prepared in PBS. Figure insets show the linear fit to oxidation current vs. 3-NT concentration.

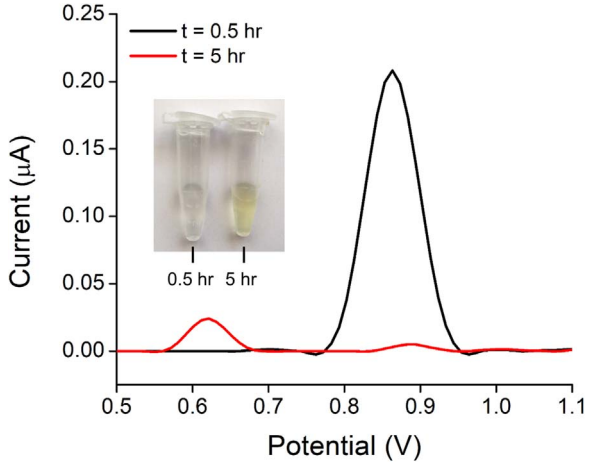

Fig. 5. Voltammogram of oxidation signals for 15 μg/mL 3-NT measured in PBS after the preparation of the solution 0.5 h. and 5 h.

In Fig. 6A, probe and hybrid coated electrodes were dipped into 20 μL of 3-NT solutions for 10 min. After 10 min, electrodes were rinsed with PBS and the potential was scanned from −0.1 V to −0.8 V. Here, 3-NT yields the largest reduction signal at −0.4 V. After interacting with probe and hybrid sequences, 3-NT reduction signal decreased in amplitude and shifted along the potential axis. For the hybrid and probe, the signal is reduced by 65% and 32%, respectively. A series of 3 repetitive measurements yield an RSD of 2.6%, 4.7%, and 1.2% for 3-NT, probe + 3-NT and hybrid + 3-NT, respectively.

In Fig. 6B, DPV measurements were monitored in ACB to measure the oxidation signal of guanine between potentials, +0.9 V and +1.10 V. We used guanine signal as a marker since guanine is an electro-active DNA base and more easily oxidized than others. Fig. 6B clearly shows that the probe sequences yield the largest signals. A dramatic reduction in the peak current of guanine bases obtained with the hybrid coated electrodes due to the hybridization. The hybridization causes a signal reduction by 88% from probe, which is due to the fact that all guanines in the probe DNA were partly closed to oxidation after hybridization. Oxidation is more difficult in the closed form compared to open form, which is due to the bases embedded in the interior of the double helix and crowded phosphate group on the helix structure. We also observed a reduction in the oxidation signal from open to closed form. Our results demonstrate that complementary target could form an entirely matched hybrid structure with the probe, resulting in a significant decrease in the magnitude of the guanine signal due to the hybridization event. After having probe and hybrid sequences on the electrode surface, the oligonucleotides coated electrodes were dipped into the 20 μL of 3-NT solution. After interacting with 3-NT, probe signal were dramatically reduced, while the hybrid signals remained unchanged. A series of three repetitive measurements

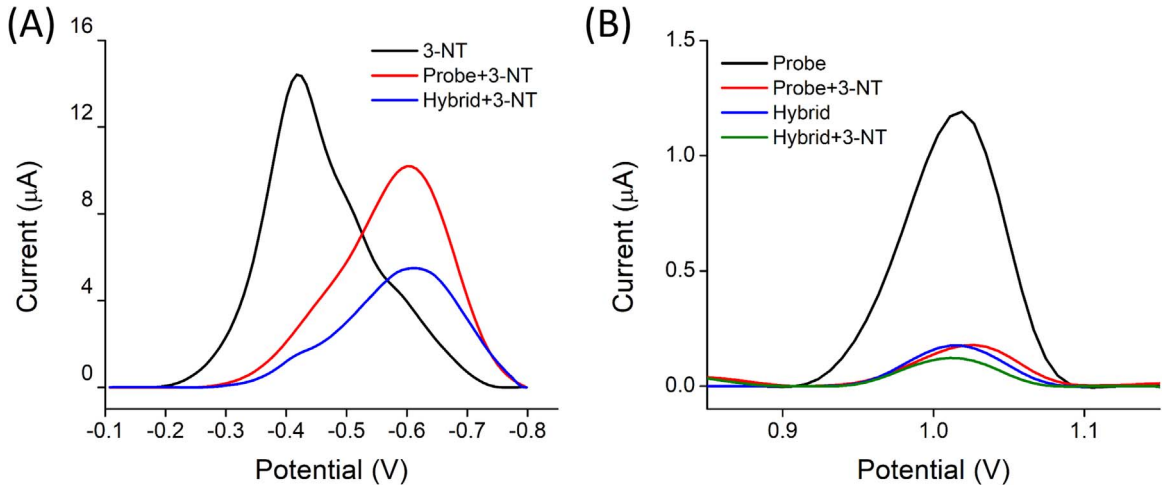

Fig. 6. Voltammograms of reduction signals of (A) 3-NT and (B) oxidation signals of guanine obtained from probe and hybrid coated PGEs. The experimental conditions are: PGEs pretreatment, 1.4 V for 30 s without stirring in ACB, 5 μg/mL probe immobilization for 20 min, interaction with 7 μg/mL target for 45 min, rinsing with PBS, interaction with 3-NT for 10 min and DPV measurement by scanning between −0.1 V and −0.8 V for reduction, and +0.7 and +1.1 V for oxidation in ACB.

of the oxidation of guanine resulted in an RSD of 4,5%, 5,9%, 2,4% and 1,1% for probe, hybrid, probe, probe + 3-NT and hybrid + 3-NT, respectively.

In interaction studies, guanine peak changes are calculated before and after the interaction to investigate the toxicity effect of chemicals on DNA with the formula below (Bagni et al., 2006). Here, S% represents the percentage of the guanine peak height change, which is the ratio of the guanine peak height after the interaction with a sample (S_s) and the guanine peak height after the interaction with the buffer solution (S_b).

$$S\% = \left(\frac{S_S}{Sb}\right)\times 100$$

A sample with $S > 85\%$ is considered as non-toxic, for $S\%$ between 50 and 85, considered as moderately toxic and $S < 50\%$, considered as toxic. The DPV signal of the biosensor in the absence of 3-NT served as 'blank', or 100%. Our results show that interaction of 3-NT with ssDNA yields an S value of 15% for probe and 80% for hybrid, which is due to the fact that 3-NT has a toxic effect on the single stranded DNA sequences (probe) and moderately toxic effect on double stranded DNA (hybrid) sequences.

4. Conclusion

Biosensor technologies are essential tools as they allow rapid, easy and low-cost analysis. In that sense, we demonstrated a new hybridization indicator, 3-NT, by utilizing both its reduction and guanine oxidation signal changes. The biosensor design consists of the immobilization of probe sequence onto the surface of a pencil graphite electrode and the target sequence was sent to the surface to create hybrid formation. After having probe and hybrid sequences onto the electrode, they were interacted with 3-NT solution. Upon the interaction with 3-NT, guanine oxidation signals of probe decreased dramatically whereas hybrid signals remain almost unchanged. The signal differences enabled us to distinguish ssDNA and dsDNA without using a label or tag. The total time of our measurements as short as 1hr., including activation of electrodes, hybridization, attachment of DNA oligonucleotides to the surface and interaction with 3-NT.

References

Acar, E.T., Onar, A.N., Onar, M.K., 2016. Investigation of electrochemical behavior and development of a validated adsorptive stripping square wave voltammetry method for 3-nitrotyrosine in human plasma and cerebrospinal fluid. J. Anal. Chem. 71 (6), 581–589.

Adhikari, B.R., Schraft, H., Chen, A.C., 2017. A high-performance enzyme entrapment platform facilitated by a cationic polymer for the efficient electrochemical sensing of ethanol. Analyst 142 (14), 2595–2602.

Afkhami, A., Hashemi, P., Bagheri, H., Salimian, J., Ahmadi, A., Madrakian, T., 2017. Impedimetic immunosensor for the label-free and direct detection of botulinum neurotoxin serotype A using Au nanoparticles/graphene-chitosan composite. Biosens. Bioelectron. 93, 124–131.

Aghaei, R., Mazloum-Ardakani, M., Abdollahi-Alibeik, M., Moshtaghioun, S.M., Rezaeipoor-Anari, A., Haghighijoo, Z., Zamani, L., 2017. A new electrochemical biosensor based on telomeric G-quadruplex DNA: in silico and experimental study of dihydropyridine derivatives potential effect on telomerase inhibition. J. Electroanal. Chem. 796, 24–32.

Aghili, Z., Nasirizadeh, N., Divsalar, A., Shoeibi, S., Yaghmaei, P., 2017. A nanobiosensor composed of exfoliated graphene oxide and gold nano-urchins, for detection of GMO products. Biosens. Bioelectron. 95, 72–80.

Alexander, S., Baraneedharan, P., Balasubrahmanyan, S., Ramaprabhu, S., 2017. Highly sensitive and selective non enzymatic electrochemical glucose sensors based on graphene oxide-molecular imprinted polymer. Mat. Sci. Eng. C-Mater. 78, 124–129.

Arevalo, F.J., Osuna-Sanchez, Y., Sandoval-Cortes, J., Di Tocco, A., Granero, A.M., Robledo, S.N., Zon, M.A., Vettorazzi, N.R., Martinez, J.L., Segura, E.P., Ilina, A., Fernandez, H., 2017. Development of an electrochemical sensor for the determination of glycerol based on glassy carbon electrodes modified with a copper oxide nanoparticles/multiwalled carbon nanotubes/pectin composite. Sens. Actuators B-Chem. 244, 949–957.

Bagni, G., Osella, D., Sturchio, E., Mascini, M., 2006. Deoxyribonucleic acid (DNA) biosensors for environmental risk assessment and drug studies. Anal. Chim. Acta 573–574, 81–89.

Bolner, A., Micciolo, R., Bosello, O., Nordera, G., 2016. A panel of oxidative stress markers in Parkinson's disease. Clin. Lab 62 (1–2), 105–112.

Chen, H.J., Chang, C.M., Lin, W.P., Cheng, D.L., Leong, M.I., 2008. H2O2/nitrite-induced post-translational modifications of human hemoglobin determined by mass spectrometry: redox regulation of tyrosine nitration and 3-nitrotyrosine reduction by antioxidants. Chembiochem 9 (2), 312–323.

Chen, H.J.C., Chen, Y.C., 2012. Reactive nitrogen oxide species-induced post-translational modifications in human hemoglobin and the association with cigarette smoking. Anal. Chem. 84 (18), 7881–7890.

Daiber, A., Munzel, T., 2012. Increased circulating levels of 3-nitrotyrosine autoantibodies marker for or maker of cardiovascular disease? Circulation 126 (20), 2371–2373.

Degendorfer, G., Chuang, C.Y., Kawasaki, H., Hammer, A., Malle, E., Yamakura, F., Davies, M.J., 2016. Peroxynitrite-mediated oxidation of plasma fibronectin. Free Radic. Biol. Med. 97, 602–615.

Dogan-Topal, B., Uslu, B., Ozkan, S.A., 2009. Voltammetric studies on the HIV-1 inhibitory drug Efavirenz: the interaction between dsDNA and drug using electrochemical DNA biosensor and adsorptive stripping voltammetric determination on disposable pencil graphite electrode. Biosens. Bioelectron. 24 (8), 2358–2364.

Erdal, N., Gurgul, S., Tamer, L., Ayaz, L., 2008. Effects of long-term exposure of extremely low frequency magnetic field on oxidative/nitrosative stress in rat liver. J. Radiat. Res. 49 (2), 181–187.

Greenacre, S.A.B., Ischiropoulos, H., 2001. Tyrosine nitration: localisation, quantification, consequences for protein function and signal transduction. Free Radic. Res. 34 (6), 541–581.

Guo, S.A., Shao, L.H., Pei, J.J., Rong, L., Wang, X.F., Chi, D.F., 2009. Determination of free 3-nitrotyrosine in human plasma using HPLC method with fluorescence detection. Chem. Anal.-Wars. 54 (4), 691–703.

Kerman, K., Vestergaard, M., Tamiya, E., 2007. Label-free electrical sensing of small-molecule inhibition on tyrosine phosphorylation. Anal. Chem. 79 (17), 6881–6885.

Kilciksiz, S., Demirel, C., Ayhan, S.E., Erdal, N., Gurgul, S., Tamer, L., Ayaz, L., 2011. N-acetylcysteine ameliorates nitrosative stress on radiation-inducible damage in rat liver. J. Buon 16 (1), 154–159.

Kilic, T., Topkaya, S.N., Ozkan Ariksoysal, D., Ozsoz, M., Ballar, P., Erac, Y., Gozen, O., 2012. Electrochemical based detection of microRNA, mir21 in breast cancer cells. Biosens. Bioelectron. 38 (1), 195–201.

Li, X.G., Li, S., Kellermann, G., 2015. A novel mixed-mode solid phase extraction coupled with LC-MS/MS for the re-evaluation of free 3-nitrotyrosine in human plasma as an oxidative stress biomarker. Talanta 140, 45–51.

Lopes, P., Dyrnesli, H., Lorenzen, N., Otzen, D., Ferapontova, E.E., 2014. Electrochemical analysis of the fibrillation of Parkinson's disease alpha-synuclein. Analyst 139 (4), 749–756.

Mahato, K., Srivastava, A., Chandra, P., 2017. Paper based diagnostics for personalized health care: emerging technologies and commercial aspects. Biosens. Bioelectron. 96, 246–259.

Ozyurt, V.H., Otles, S., 2017. Determination of 3-nitrotyrosine in food protein suspensions. Talanta 171, 81–89.

Radi, R., 2013. Protein tyrosine nitration: biochemical mechanisms and structural basis of functional effects. Acc. Chem. Res. 46 (2), 550–559.

Richards, D.A., Silva, M.A., Devall, A.J., 2006. Electrochemical detection of free 3-nitrotyrosine: application to microdialysis studies. Anal. Biochem. 351 (1), 77–83.

Roy, E., Patra, S., Madhuri, R., Sharma, P.K., 2015. Developing electrochemical sensor for point-of-care diagnostics of oxidative stress marker using imprinted bimetallic Fe/Pd nanoparticle. Talanta 132, 406–415.

Sharov, V.S., Galeva, N.A., Kanski, J., Williams, T.D., Schoneich, C., 2006. Age-associated tyrosine nitration of rat skeletal muscle glycogen phosphorylase b: characterization by HPLC-nanoelectrospray-tandem mass spectrometry. Exp. Gerontol. 41 (4), 407–416.

Sun, Y.C., Chang, P.Y., Tsao, K.C., Wu, T.L., Sun, C.F., Wu, L.L., Wu, J.T., 2007. Establishment of a sandwich ELISA using commercial antibody for plasma or serum 3-nitrotyrosine (3NT). Elevation in inflammatory diseases and complementary between 3NT and myeloperoxidase. Clin. Chim. Acta 378 (1–2), 175–180.

Teixeira, D., Prudencio, C., Vieira, M., 2017. Development of a new HPLC-based method for 3-nitrotyrosine quantification in different biological matrices. J. Chromatogr. B 1046, 48–57.

Topkaya, S.N., Aydinlik, S., Aladag, N., Ozsoz, M., Ozkan-Ariksoysal, D., 2010. Different DNA immobilization strategies for the interaction of anticancer drug irinotecan with DNA based on electrochemical DNA biosensors. Comb. Chem. High. Throughput Screen 13 (7), 582–589.

Topkaya, S.N., Kosova, B., Ozsoz, M., 2014. Detection of Janus Kinase 2 gene single point mutation in real samples with electrochemical DNA biosensor. Clin. Chim. Acta 429, 134–139.

Topkaya, S.N., Ozkan-Ariksoysal, D., Kosova, B., Ozel, R., Ozsoz, M., 2012. Electrochemical DNA biosensor for detecting cancer biomarker related to glutathione S-transferase P1 (GSTP1) hypermethylation in real samples. Biosens. Bioelectron. 31 (1), 516–522.

Wang, Z., Paik, D.C., Dillon, J.P., Gaillard, E.R., 2007. Tyrosine nitration site specificity identified by LC/MS in nitrite-modified collagen type IV. Exp. Mol. Med. 39 (1), 74–83.

Weber, D., Kneschke, N., Grimm, S., Bergheim, I., Breusing, N., Grune, T., 2012. Rapid and sensitive determination of protein-nitrotyrosine by ELISA: application to human plasma. Free Radic. Res. 46 (3), 276–285.

Yokoyama, K., Uhlin, U., Stubbe, J., 2010. Site-specific incorporation of 3-nitrotyrosine as a probe of pKa perturbation of redox-active tyrosines in ribonucleotide reductase. J. Am. Chem. Soc. 132 (24), 8385–8397.

Zhao, Z., Zhou, H., Peng, Y., Qiu, C.H., Sun, Q.Y., Wang, F., Xie, H.N., 2014. Expression and significance of plasma 3-NT and ox-LDL in patients with Alzheimer's disease. Genet. Mol. Res. 13 (4), 8428–8435.